Journal of Alloys and Compounds 509 (2011) L324–L327

Contents lists available at ScienceDirect

Journal of Alloys and Compounds

journal homepage: www.elsevier.com/locate/jallcom

Letter

Synthesis of in situ network-like vapor-grown carbon fiber improved $LiFePO_4$ cathode materials by microwave pyrolysis chemical vapor deposition

F. Deng [a], X.R. Zeng [b,c,*], J.Z. Zou [b,c], J.F. Huang [c], X.B. Xiong [b,c], X.H. Li [b,c]

[a] School of Materials Science and Engineering, Northwestern Polytechnical University, Xi' an 710072, China
[b] College of Materials Science and Engineering, Shenzhen University, Shenzhen 518060, China
[c] Shenzhen Key Laboratory of Special Functional Materials, Shenzhen 518060, China

ARTICLE INFO

Article history:
Received 7 September 2010
Received in revised form 6 June 2011
Accepted 14 June 2011
Available online 29 June 2011

Keywords:
Electrode materials
Gas–solid reactions
Vapor deposition
Microstructure
Scanning electron microscopy

ABSTRACT

The low electronic conductivity of $LiFePO_4$ currently limits its use in lithium ion batteries. In order to solve the problem, in situ network-like vapor-grown carbon fiber (VGCF) improved $LiFePO_4$ cathode materials have been prepared in one step by microwave pyrolysis chemical vapor deposition. The phase, microstructure and electrochemical performances of the composites were investigated. Compared with the cathodes without in situ VGCF, the initial discharge capacity of the composite electrode increases from 84 mAh g^{-1} to 123 mAh g^{-1} at 3.0 C rate, and the charge transfer resistance varies from 420 Ω to 75 Ω. The possible reasons of those are proposed.

1. Introduction

$LiFePO_4$ (LFP) could be used as cathode material for lithium ion batteries because of its large theoretical capacity of 170 mAh g^{-1}, good thermal stability in fully charged state and little hygroscopic. In addition, this material is inexpensive, nontoxic, and environmentally benign [1–3]. However, the electronic conductivity of pure LFP (10^{-10} to 10^{-9} S cm^{-1} [4]) is by several orders of magnitude lower than that of other important cathode materials (~10^{-3} S cm^{-1} for $LiCoO_2$ [5] or 10^{-4} S cm^{-1} for $LiMn_2O_4$ [6]). Therefore, lattice doping [4] or surface coating methods [7–10] have been conducted to overcome the weakness.

Because of excellent mechanical properties, high electrical and thermal conductivity, vapor-grown carbon fiber (VGCF) has been reported as ideal conductive fillers in different electrodes [11–13]. Chen et al. [14] reported that the first discharge capacity of VGCF enhanced LFP composite was more than 2 times of those without VGCF. Nevertheless, ball milling, as the most selected way to introduce conductive additives in the mixing process, could inevitably damage their initial structure and increase the contact resistance between additives [14–16].

Higuchi et al. were the first to apply microwave in the preparation of LFP [17]. Microwave could ensure uniform and fast heating through a self-heating process based on direct microwave energy absorption by the materials [18]. Microwave pyrolysis chemical vapor deposition (MCVD) has ever been used to obtain VGCF in our previous work [19]. In this paper, MCVD technology was developed to synthesize in situ network-like VGCF improved LFP cathode materials in order to enhance its electronic conductivity.

2. Experimental

2.1. Synthesis

$FeC_2O_4{\cdot}2H_2O$, $NH_4H_2PO_4$, and $LiOH{\cdot}H_2O$ with mole ratio 1:1:1 were dispersed into 75 wt% (compared to the raw materials) absolute ethyl alcohol, and then 5.4 wt% carbon black (SuperP Erachem) was added into it. The mixture was mixed by ball-milling in a Spex-8000 ball at 300 rpm for 6 h. After dried under vacuum at 120 °C for 12 h, the samples were placed in a home-made quartz reactor installed in the MCVD equipment [20] (Fig. 1). After filled with argon, the equipment was set at a microwave output power of 800 W. One kind of samples, designated as "VC/LFP", was prepared at a temperature range of 550–800 °C. When the temperature reached the setting value, propylene with a flow of 90 sccm was put into the quartz reactor for 10 min, and then the MCVD equipment was closed. For comparison, another kind of samples, designated as "C/LFP", was also obtained at the same conditions except no participation of propylene in the synthetic process.

2.2. Characterization

The X-ray powder diffraction (XRD, D8 ADVANCE, Bruker AXS) with Cu Kα radiation was used to identify the phases. An integrated Raman microscope system (inVia Reflex, Renishaw) was used to analyze the structure and composition. The excitation wavelength was supplied by an internal Ar (514.5 nm) 20 mW laser. Field emission scanning electron microscope (FESEM, S-4800, HITACHI) and energy dispersive X-

* Corresponding author. Tel.: +86 755 26557459; fax: +86 755 26536239.
E-mail address: zengxier@szu.edu.cn (X.R. Zeng).

0925-8388/$ – see front matter
doi:10.1016/j.jallcom.2011.06.054

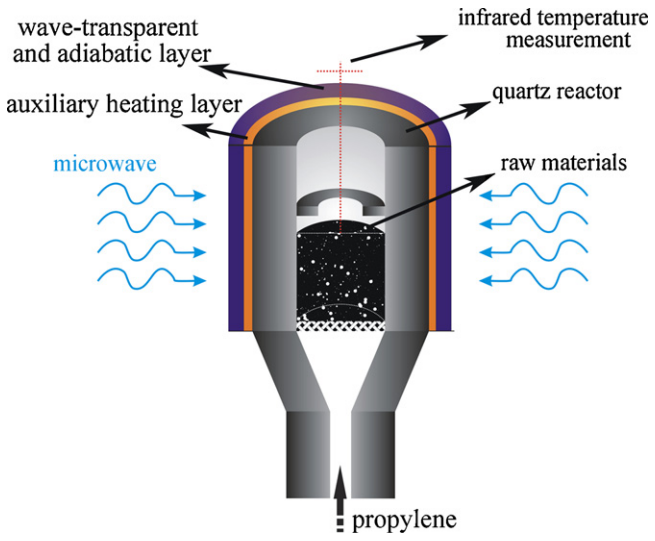

Fig. 1. Sketch of the MCVD reactor.

ray spectroscopy (EDS, EDAX) were used to analyze the morphology and elementary component, respectively.

2.3. Electrochemical properties

The cathodes containing 95 wt% active materials and 5 wt% polyvinylidene fluoride (PVDF) were prepared by spreading a slurry in N-methylpyrrolidone (NMP) onto aluminum foil current collectors and allowing them to dry. 2032 size coin cells were assembled in an argon-filled glove box, using lithium as a counter electrode and 1 M $LiPF_6$ in 1:2 ethylene carbonate/dimethyl carbonate (EC/DMC) electrolyte solution. Charge/discharge tests were performed using an Arbin Instrument (BT2000) at 25 °C. The electrochemical impedance spectroscopy (EIS) was measured with a frequency response analyzer (Solatron 1260) interfaced with a potentio-galvanostat (Solatron 1287). The sinusoidal excitation voltage applied to the cells was 10 mV with a frequency range from 100 kHz to 10 mHz. We analyzed the impedance data to evaluate the equivalent circuit parameters by using a parameter fitting program (Scribner Associates, Zplot for Windows).

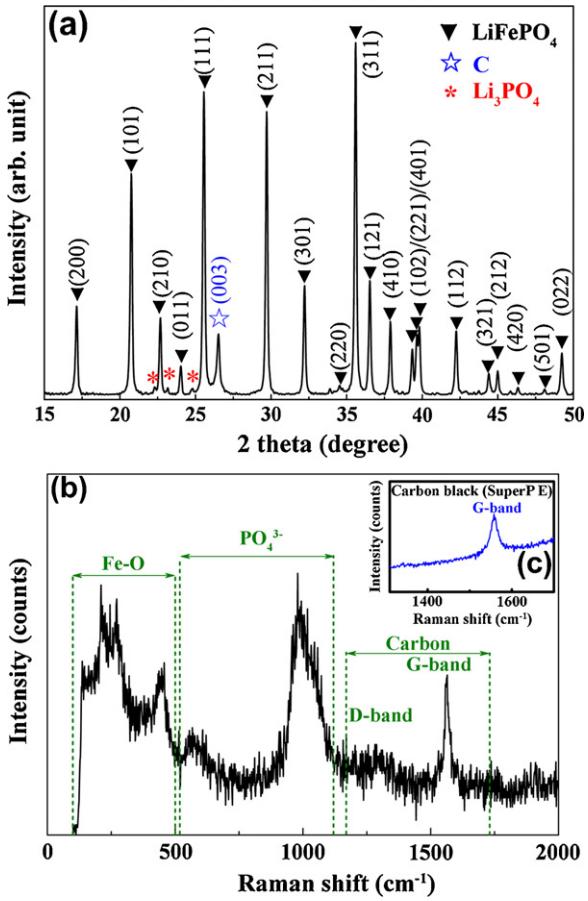

Fig. 2. (a) XRD profile and (b) Raman spectrum of VC/LFP synthesized by MCVD at 650 °C. (c) Raman spectrum of carbon black used in the raw materials.

3. Results and discussion

The XRD profile shown in Fig. 2a of VC/LFP can be indexed to a major phase of orthorhombic LFP (JCPDS: 83-2092) and a minor phase of rhombohedral graphite-3R (JCPDS: 26-1079), except for several weak diffraction peaks of orthorhombic Li_3PO_4 (JCPDS:

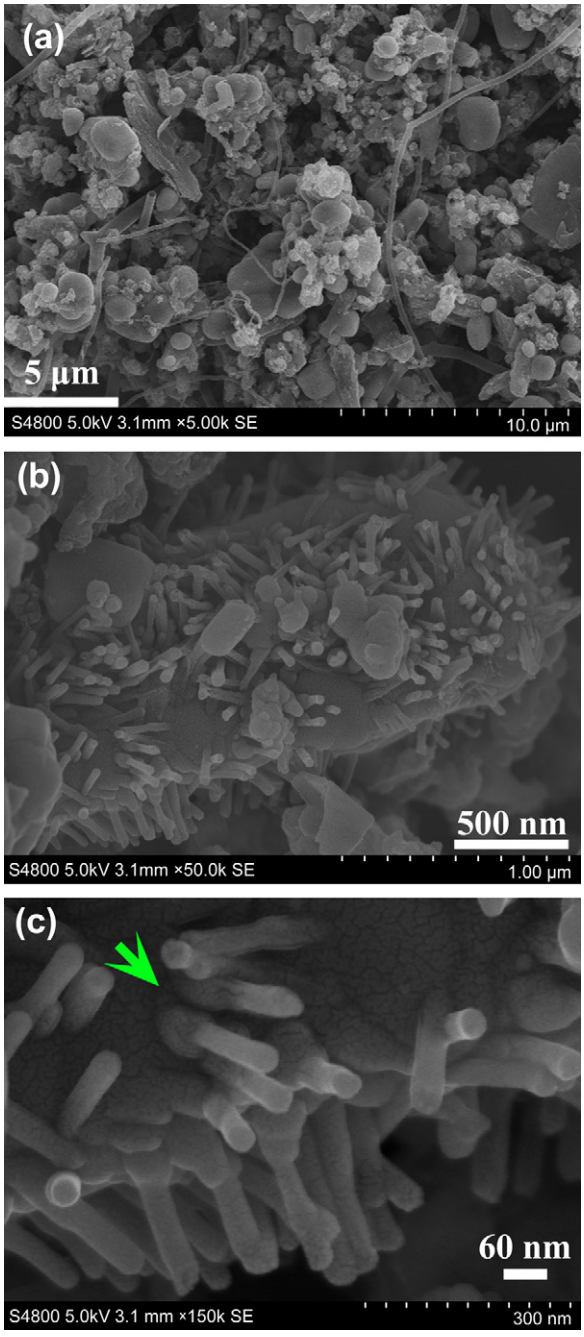

Fig. 3. (a) Typical FESEM image of VC/LFP synthesized by MCVD at 700 °C, (b) FESEM morphology of VGCF observed on the surface of graphite particles in VC/LFP obtained by MCVD at 600 °C, and (c) higher magnification of (b).

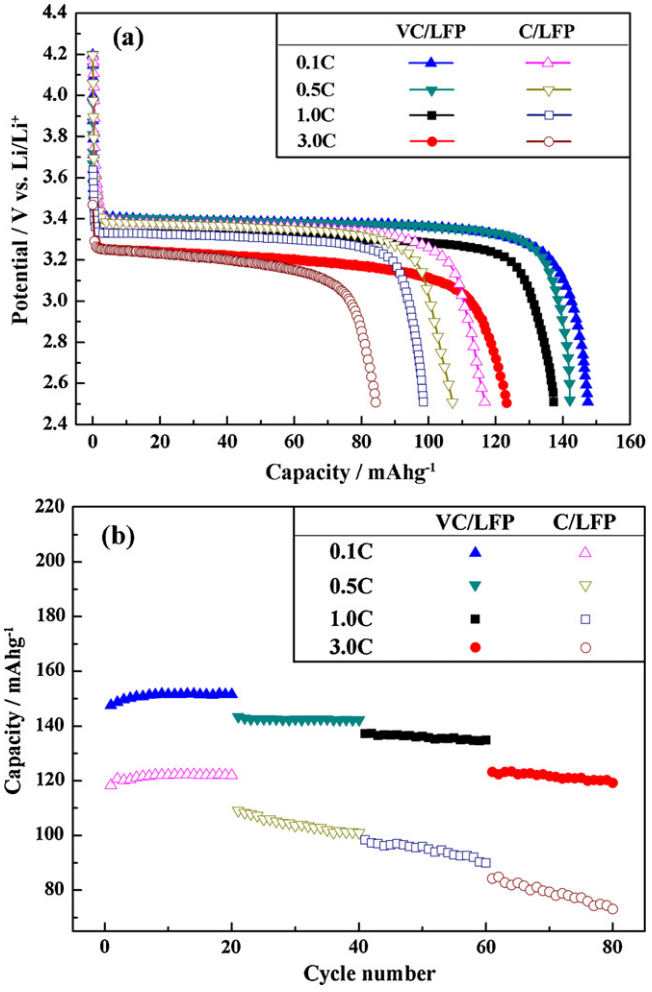

Fig. 4. (a) Discharge curves and (b) cycling performance of VC/LFP and C/LFP (both obtained by MCVD at 650 °C) cathodes measured with different rates at 25 °C.

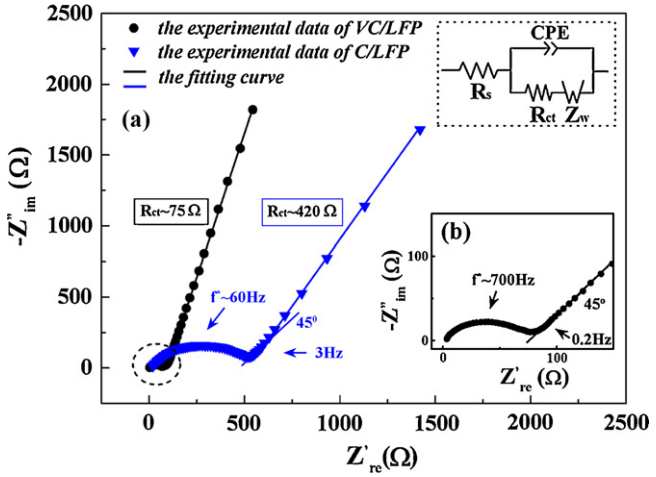

Fig. 5. (a) Electrochemical impedance spectra of VC/LFP and C/LFP (both obtained by MCVD at 650 °C) composite cathodes and (b) partial enlarged impedance spectrum of VC/LFP sketched by the elliptic dashed zone shown in (a).

15-0760). The mean crystallite size of LFP is ~72 nm, calculated from the widths of the major diffraction peaks of (2 0 0), (1 0 1), and (3 1 1) by Scherrer's formula. The diffraction peaks of graphite are resulted from the carbon black mixed in the raw materials. The phase content of LFP, C, and Li_3PO_4, calculated by semiquantitative method of relative intensity to reference, are ~84 wt%, ~14.5 wt%, and ~1.5 wt%, respectively. The Raman spectra of VC/LFP and carbon black used in the raw materials are shown in Fig. 2b and c. The bands at 500–100 cm^{-1} and 1120–520 cm^{-1} correspond to the Raman vibrations of Fe–O and PO_4^{3-} in LFP, respectively [21], while the bands in the range of 1460–1170 cm^{-1} and 1730–1470 cm^{-1} can be assigned to the D-band (disorder-induced phonon mode) and G-band (graphite band) of carbon, respectively. Compared with the Raman spectrum of carbon black used in the raw materials, the ratio of D/G integrated peak intensities is increased appreciably.

The typical FESEM morphology shown in Fig. 3a and EDS analyses (not shown here) of VC/LFP indicate that the VC/LFP is composed of sphere-like LFP, flaky graphite, and network-like fibers. Noticeably, most VGCF shown in Fig. 3b grow on the surface of graphite particles, and further magnified image shown in Fig. 3c reveals an in situ growth mode. The in situ formation of VGCF could be attributed to the pyrolysis and deposition of propylene under special effect of microwave heating and/or the self-catalytic action of something (e.g. $FeC_2O_4{\cdot}2H_2O$) in the raw materials. In addition, the turbostratic graphite generally formed on the near-surface of VGCF [13] may give some clues to interpret the weak D-band in the Raman spectrum (see Fig. 2b).

The electrochemical performance of VC/LFP cathodes is better than that of C/LFP cathodes (Fig. 4). The initial discharge capacity of the VC/LFP cathodes is 148 mAh g^{-1} at 0.1 C rate, 144 mAh g^{-1} at 0.5 C rate, 137 mAh g^{-1} at 1.0 C rate and 123 mAh g^{-1} at 3.0 C rate, which are slightly better than those of some other materials [14]. Furthermore, the capacity fading on cycling VC/LFP cathodes is surprisingly negligible.

Fig. 5 compares the electrochemical impedance spectra of VC/LFP and C/LFP composite electrodes. Both Nyquist plots exhibit a semicircle at high frequencies followed by a sloping line at medium frequencies. At very low frequencies the phase angle begins to increase due to the onset of finite length effects [22]. The interpretation of the impedance spectra is based on the equivalent circuit shown in Fig. 5 where R_s represents the sum of the ohmic resistance of the research system, CPE (constant phase element) represents the double layer capacitance and the SEI (solid electrolyte interface) film capacitance instead of a capacitor to compensate for nonhomogeneity in the system, R_{ct} is a charge transfer resistor which is related to the electrochemical reaction at the electrode–electrolyte interface and particle–particle contact and Z_W is the Warburg impedance which is associated with the lithium ion diffusion in the bulk of the active material [23–25]. A decrease in the charge transfer resistance from 420 Ω in the C/LFP composite electrode to 75 Ω in the VC/LFP composite electrode is related to the improvement in electronic conductivity provided by the network-like VGCF, facilitating faster charge transfer between the electrolyte and the $LiFePO_4$ particles. This is also supported by the changes in electrochemical performance as discussed above (Fig. 4).

4. Conclusions

In situ VGCF improved $LiFePO_4$ composite cathode materials for lithium ion batteries can be prepared by a MCVD process in the temperature range between 550 °C and 800 °C. As a result of the formation of network-like VGCF in the as-prepared materials, $LiFePO_4$ composite cathode materials show better electrochemical properties in relation to rate capacity and cycling life. This work demonstrates a novel approach for preparing high-performance $LiFePO_4$ cathode materials for high power lithium ion batteries.

Acknowledgements

This work was supported by the Two Hundred Plan for Talent Station of Shenzhen (Shenfu [2008] No. 182), the Science and

Technology R&D Program of Shenzhen (CXB201005240010A and ZD200904290044A), the Science and Technology Project of Shenzhen (JC200903130266A) and the fund of Shenzhen Key Laboratory of Special Functional Materials (T201005). We also thank Professor Wenjun Liu for his technical guidance with electrochemical impedance spectroscopy.

References

[1] A.K. Padhi, K.S. Najundaswamy, J.B. Goodenough, J. Electrochem. Soc. 144 (1997) 1188.
[2] A.K. Padhi, K.S. Najundaswamy, C. Masquelier, S. Okada, J.B. Goodenough, J. Electrochem. Soc. 144 (1997) 1609.
[3] A.K. Padhi, K.S. Najundaswamy, C. Masquelier, J.B. Goodenough, J. Electrochem. Soc. 144 (1997) 2581.
[4] S.Y. Chung, J.T. Bloking, Y.M. Chiang, Nat. Mater. 1 (2002) 123.
[5] J. Molenda, A. Stoklosa, T. Bak, Solid State Ionics 36 (1989) 53.
[6] J. Guan, M. Liu, Solid State Ionics 110 (1998) 21.
[7] H. Huang, S.C. Yin, L.F. Nazar, Electrochem. Solid State Lett. 4 (2001) A170.
[8] N. Ravet, J.B. Goodenough, S. Besner, M. Simoneau, P. Hovington, M. Armand, 196th Meeting Abstract of the Electrochemical Society, Hawaii, USA, 1999, p. 127.
[9] I. Belharouak, C. Johnson, K. Amine, Electrochem. Commun. 7 (2005) 983.
[10] F. Croce, A.D. Epifanio, J. Hassoun, A. Deptula, T. Olczac, B. Scrosatia, Electrochem. Solid State Lett. 5 (2002) A47.
[11] K. Tatsumi, K. Zaghib, Y. Sawada, H. Abe, T. Ohsaki, J. Electrochem. Soc. 142 (1995) 1090.
[12] M. Endo, Y. Nishimura, T. Takahashis, K. Takeuchi, M.S. Dresselhaus, J. Phys. Chem. Solids 57 (1996) 725.
[13] M. Endo, Y.A. Kim, T. Hayashi, K. Nishimurab, T. Matusitaa, K. Miyashitaa, Carbon 39 (2001) 1287.
[14] C.C. Chen, M.H. Liu, J.M. Chen, 206th meeting of the Electrochemical Society, Hawaii, USA, 2004, p. 413.
[15] X.L. Li, F.Y. Kang, X.D. Bai, W.C. Shen, Electrochem. Commun. 9 (2007) 663.
[16] B. Jin, E.M. Jin, K.H. Park, H.B. Gu, Electrochem. Commun. 10 (2008) 1537.
[17] M. Higuchi, K. Katayama, Y. Azuma, M. Yukawa, M. Suhara, J. Power Sources 119–121 (2003) 258.
[18] K.S. Park, J.T. Son, H.T. Chung, S.J. Kim, C.H. Kim, C.H. Lee, Electrochem. Commun. 5 (2003) 839.
[19] J.Z. Zou, X.R. Zeng, X.B. Xiong, H.L. Tang, L. Li, Q. Liu, Carbon 45 (2007) 828.
[20] X.R. Zeng, F. Deng, J.Z. Zou, CN Patent 200910110427.6 (2010).
[21] C.M. Burba, R. Frech, J. Electrochem. Soc. 151 (2004) A1032.
[22] C. Ho, I.D. Raistrick, R.A. Huggins, J. Electrochem. Soc. 127 (1980) 343.
[23] Y.K. Zhou, B.L. He, W.J. Zhou, H.L. Li, J. Electrochem. Soc. 151 (2004) A1052.
[24] C.Y. Lee, H.M. Tsai, H.J. Chuang, S.Y. Li, P. Lin, T.Y. Tseng, J. Electrochem. Soc. 152 (2005) A716.
[25] Y.M. Choia, S.I. Pyun, Solid State Ionics 99 (1997) 173.